

Demibootstrap approach to hadron-spectrum dynamics

Louis A. P. Balázs

Physics Department, Purdue University, West Lafayette, Indiana 47907

(Received 17 March 1986)

A “demibootstrap” approach is proposed in which long-range “open” hadronic-channel corrections to a primordial short-range valence-quark (or parton) model are calculated nonperturbatively and self-consistently. These open channels are found to provide most of the dynamics generating the leading Regge-trajectory hadron spectrum and lead to good agreement with experiment. Some of our methods may perhaps be applicable in implementing the compactification of superstrings.

In most practical mass-spectrum calculations based on quantum chromodynamics (QCD), the force between valence quarks (q), diquarks (qq), or gluons (G) is assumed, in first approximation, to arise from a stable narrow rotating flux tube (or string) formed by the nonperturbative exchange of gluons; this becomes approximately spherical for ground states and can presumably be approximated by a bag model. The effect of $q\bar{q}$ creation (annihilation)—leading to the fragmentation (reformation) of the flux tube—is neglected. This is the attitude adopted in the quenched lattice approach and in the $1/N_{\text{color}}$ expansion, for example, where such $q\bar{q}$ effects are supposed to come in only as higher-order corrections; it leads to a universal string tension and Regge slope, at least for higher angular momentum.

In practice, however, explicit Skyrme-model¹ and quenched q -loop lattice calculations² seem to give consistently larger N - ρ mass ratios and smaller Δ - N mass differences than are warranted by experiment, and there is an increasing accumulation of evidence that the effect of $q\bar{q}$ creation is anything but negligible. In particular, the controlling expansion parameter in a realistic $1/N_{\text{color}}$ expansion turns out to be, not $1/N_{\text{color}}$ itself, but rather, $N_{\text{flavor}}/N_{\text{color}}$, which is effectively of order unity in the real world. Moreover, interquark flux tubes are known to fission quite readily in jet-formation experiments, typical hadronic couplings are known to be quite large experimentally, and the inclusion of hadronic channels is known to lead to important mass shifts in explicit hadron-mass calculations;³ all of these are a consequence of $q\bar{q}$ creation, which also turns out to be quite important in recent explicit field-theory model estimates.⁴

The dynamical effect of $q\bar{q}$ creation seems to be particularly important at moderately long-range interquark “confinement” region distances. In deep-inelastic lepton-hadron scattering, for example, “sea” quarks, which arise from $q\bar{q}$ creation, give a major contribution for smaller momentum fractions (or Feynman- x values) within hadrons—precisely the x region which corresponds to smaller energies and hence larger distances within the hadron rest frame. Calculations which ignore $q\bar{q}$ creation also have problems with chiral symmetry, and in accounting for the smallness of the pion mass. The phenomenological “chiral bag” or “cloudy bag” way of overcoming such difficulties has been to assume a peripheral cloud of mesons around a core of valence quarks.⁵ But this is

clearly reconcilable with QCD only if we assume that the “hadronization” arising from $q\bar{q}$ creation is a non-negligible part of “confinement” dynamics.

We have therefore embarked on a program in which such hadronization is assumed to play an important non-perturbative role from the beginning. In effect, we use a bootstraplke approach of the type proposed originally by Gell-Mann, in which we try to generate a self-consistent S matrix, but with high-momentum (short-range) boundary conditions (taken, e.g., from QCD) imposed on the theory.⁶

We start from Fig. 1, or any other short-range valence-quark or parton theory. This gives a zeroth-order hadronic spectrum (H_0) which could itself be calculated, in principle, by using quenched lattice methods (from “fundamental” QCD parameters) or some variant of the bag model (from more phenomenological parameters). In this respect our approach resembles the $1/N_{\text{color}}$ expansion or the hadronic Skyrme and static strong-coupling models,^{1,7} as well as various more phenomenological perturbative or semiperturbative hadron-loop mass-correction schemes.³ However, it differs from these in that it uses truly nonperturbative S -matrix methods to build up the hadron-channel contributions arising from the addition of (planar) quark loops to Fig. 1. Such graphs lead to the generalized hadronic ladder sums of Fig. 2 (Ref. 8), where the H “ladders” within Figs. 2(b), 2(c), . . . should themselves have the form of the entire sum of Fig. 2, which leads to output Regge trajectories $\alpha(t = m^2)$ interpolating physical hadron (H) masses m . Nonplanar graphs can be treated as corrections.⁸

Since sea quarks appear to be important primarily at longer distances, as we have seen, we will assume that the vertical lines (W) of Fig. 2 are dominated by H contributions for low-mass $m < m_c$ (peripheral) exchanges and by the H_0 of Fig. 1 for high-mass $m > m_c$ (short-range) exchanges. Regge-resonance duality permits us to replace the latter by horizontal H_0 Regge (α_0) lines, so that Fig.

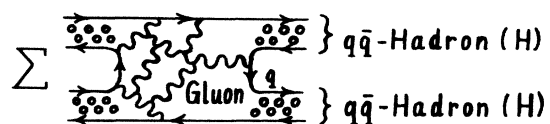


FIG. 1. Planar amplitude without internal q loops.

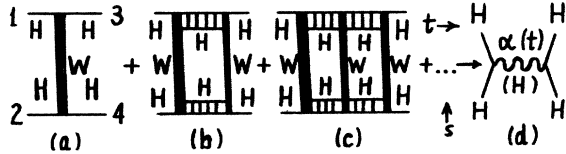


FIG. 2. Hadron-line version of Fig. 1 with internal q loops.

2(a) reduces to Fig. 3. By contrast, Ref. 3 would in effect simply drop Fig. 3(b) and make crude one-particle approximations for the H_0 exchange of Fig. 3(c) and the H ladders of Figs. 2(b), 2(c), It is doubtful whether such a few-channel approximation is adequate for what is basically an infinite-channel problem, however. On the other hand, it was Fig. 3(c) which was dropped in Ref. 8. While Fig. 3(c) is indeed a small contribution, as we shall see, both Figs. 3(b) and 3(c) will be retained in what follows.

We will formally associate a coupling parameter ϕ with each of the W exchanges of Fig. 2 and take the Mellin-transform projection⁸

$$A_j(t) = \int_0^\infty ds v^{-j-1} A(s, t) \tag{1}$$

of the s -channel absorptive part $A(s, t)$ ($=\text{Im}T$ for $t < 0$), where s, t, u are the usual Mandelstam variables and v is the usual crossing-symmetry variable $(s - u)/2$, or

$$v = s + \frac{1}{2} \left[t - \sum m_i^2 \right], \tag{2}$$

with m_i equal to the masses of the external lines $i = 1, 2, 3, 4$. If we take the [1,1] Padé approximant of the resulting expansion in ϕ , we obtain

$$A_j(t) = W_j(t) / [1 - B_j(t) / W_j(t)], \tag{3}$$

where W and B are the contributions of Figs. 2(a) and 2(b). The optimum m_c would then be the highest value which avoids double counting between Figs. 3(b) and 2(b) (and thus also between quark and hadron degrees of freedom).

Equation (3) is exact if we have a factorizable model⁸

$$\bar{y}^{\alpha_1+1-S_m} / (\alpha_1+1-S_m) = \left[\int_{\bar{y}}^\infty dy y^{-\alpha_1-1} \ln y G(y) \right] / \left[\int_{\bar{y}}^\infty dy y^{-\alpha_1-1} G(y) \right], \tag{8}$$

where $\bar{y} = \bar{v}/v_a$, $y = v/v_a$, $G = v_a \Lambda(s, t) / \Gamma(t)$, and (\bar{v}, v_k) are Eq. (2) at $s = (\bar{s}, m_k^2)$; we took $\Lambda = 0$ for $s < \bar{s}$ to avoid L - Λ double counting.

In the case of planar graphs such as Fig. 2(b), it is well known that the familiar two-Reggeon j -plane cut does not

FIG. 3. Low-mass $m = \sqrt{s} < m_c$ (peripheral) and high-mass $m = \sqrt{s} > m_c$ (short-range) contributions to Fig. 2(a).

with, e.g., the projected Figs. 2(b), 2(c), etc., giving $W_j k_j W_j, W_j k_j W_j k_j W_j$, etc., where k is related to a loop integral. This kind of structure arises quite naturally, at least approximately, from the factorizable Regge-exchange diagrams 3(c) and 2(d) combined with average duality, which relates the latter to the contribution of Fig. 3(b). It then also gives

$$B_j(t) / W_j(t) = [1 + I_j(t) / L_j(t)] \Lambda_j(t) / L_j(t), \tag{4}$$

where I is given by Fig. 3(c), whereas L and Λ are given by Figs. 2(a) and 2(b), but with the contribution of Fig. 3(c) to the vertical W lines set equal to zero.

Suppose we assume that the vertical-line exchange of Fig. 3(b) can be approximated by a single (average) mass m_a , so its contribution to $W(s, t)$ is

$$L(s, t) = \Gamma(t) \delta(s - m_a^2), \tag{5}$$

where $\Gamma(t)$ is typically proportional to a polynomial in t . Assuming leading-Regge dominance, Fig. 3(c) gives

$$I(s, t) = \beta_0(t) v^{\alpha_0(t)} \theta(s - m_c^2), \tag{6}$$

where $\alpha_0(t)$ and $\beta_0(t)$ can be extracted from quenched-lattice calculations.

If we drop the contribution I_j of Fig. 3(c) in Eq. (4), a vanishing of the denominator of Eq. (3) for the resulting first-approximation amplitude $A_j^1(t)$ leads to a j -plane Regge pole at $j = \alpha_1(t)$ with residue $\beta_1(t)$. The amplitude A^1 is, of course, intrinsically non-crossing-symmetric. Since it only involves long-range (low- s) "soft" dynamics without any high-mass scale, however, semilocal duality between the a exchange in Eq. (5) or Fig. 3(b) and the α_1 Regge behavior $b_1 v^{\alpha_1}$ of A_1 is expected to be more valid than any similar relation for A itself, which also has a high-mass scale coming from Fig. 3(c). We therefore have the finite-energy sum rule (FESR):

$$\int_0^{\bar{s}} ds [L(s, t) - \beta_1(t) v^{\alpha_1(t)} \theta(v)] v^{-S_m} = 0, \tag{7}$$

with $S_m = \max(S_1 + S_2, S_3 + S_4)$ and an \bar{s} midway between $[a]$ and its first Regge recurrence. Equations (3), (5), and (7) then give

appear on the physical sheet, and that there is, instead, a sharp falloff in s (or y) for large s (Ref. 8). We therefore expect a peaking of $y^{-\lambda} G(y)$ with an appropriate α_1 -independent λ . We can therefore expand⁸

$$\ln y = \ln y_1 + y_1^{-1} (y - y_1) - \frac{1}{2} y_1^{-2} (y - y_1)^2 + \dots \tag{9}$$

within Eq. (8), with an α_1 -independent peak position $y = y_1$ and λ such that $g_1 = 0$, where

$$g_n = \int_{\bar{y}}^\infty dy G(y) y^{-\lambda} (y - y_1)^n. \tag{10}$$

We will assume that the dynamics requires y_1 (and hence the corresponding s_1) to take on the lowest value capable of giving a solution for α_1 from Eq. (8), which then gives

$$\alpha_1(t) = S_m - 1 + \frac{1}{\ln \bar{y}} \left[1 - \frac{1}{e(\ln \bar{y})^2} y_1^{-2} g_2 / g_0 \right]. \quad (11)$$

This minimum $y_1 (\simeq \bar{y}^\epsilon)$, which is also the only one giving a unique α_1 , corresponds to the highest s -channel production multiplicity of the W of Fig. 2 when we expand Eq. (3) in powers of B_j/W_j and take its inverse Mellin transform to obtain $A^{(s,t)}$ (Refs. 8 and 9). In a string picture this would be equivalent to maximizing the breaking of the string as it is stretched. Since the energy of an unbroken string rises rapidly with length, such maximal breaking corresponds to a minimization of the energy in the s channel.

If we assume that $y^{-\lambda} G(y)$ is proportional to a universal function $U(u)$ of $u = (y - y_1)/(y_1 - \bar{y})$, then $y_1^{-2} g_2 / g_0 \simeq c(1 - \bar{y}^{1-\epsilon})^2$.

In dealing with the short-range contributions I_j of Fig. 3(c) in Eq. (4), we need a model for the t dependence of β_0 and α_0 in Eq. (6). Eventually this would arise from some fundamental short-range theory, such as a quenched-lattice calculation. Since an adequate and reliable theory of this type does not as yet exist, we shall, instead, follow the kind of arguments sometimes made in connection with the $1/N_{\text{color}}$ expansion, and assume that Fig. 1 gives an amplitude T_0 satisfying a dual resonance (string) model. This would require a linear $\alpha_0(t)$, and should lead to approximate semilocal FESR duality:

$$\int_0^{\bar{s}_0} ds [\Gamma_0(t) \delta(s - m_0^2) - \beta_0(t) v^{\alpha_0(t)} \theta(v)] v^{-S_m} = 0, \quad (12)$$

where $\Gamma_0(t)$ is proportional to a polynomial in t of the same order as $\Gamma(t)$ and arises from the lowest s -channel exchange (of mass m_0) of Fig. 1. Physically, α_0' is then universal, as we have seen.

Equation (3) now has a Regge pole at $j = \alpha$ arising from the vanishing of its denominator when $B_j = W_j$ with $I_j \neq 0$. If we combine this with Eq. (12) and our first-approximation $I_j = 0$ results, we obtain the correction

$$\alpha(t) - \alpha_1(t) = \frac{1}{e \ln \bar{y}} \frac{\alpha_0 + 1 - S_m}{\alpha_0 - \alpha} \left[\frac{\bar{v}_0}{v_0} \right]^{S_m} \left[\frac{\bar{v}_0}{v_c} \right]^{-\alpha_0 - 1} \times \left[\frac{v_c}{v_a} \right]^{-\alpha - 1} \left[\frac{\Gamma_0(t)}{\Gamma(t)} \right]. \quad (13)$$

For $v_a > 0$, we can now expand Eqs. (11) and (13) in powers of v_a^{-1} to get

$$\alpha(t) = 2\hat{\alpha}' v_a + S_m + c + p_1 v_a^{-1} + p_2 v_a^{-2} + \dots \quad (14)$$

Equations (13) and (11) give branch points at $v_a = 0$, $-(\bar{s} - s_a)$, $-(\bar{s}_0 - s_a)$, and $-(s_c - s_a)$, where $s_a = m_a^2$. In Ref. 8 it was argued that such singularities are spurious and that Eqs. (13) and (11) break down in the regions where they occur. Away from these regions, however, $\alpha(t)$ can be well approximated by the large $-v_a$ form (14) with $p_i = 0$.

The results (13) and (14) apply to an infinite number of processes with the same α . For example, we should have the same output α_ρ both in $\rho\rho \rightarrow \rho\rho$ and $\rho'\rho' \rightarrow \rho\rho$, where ρ' is any Regge recurrence of ρ . Now the linear $-\alpha(t)$ form (14) with $p_i = 0$ continues to apply in a region of in-

validity of Eqs. (13) and (11) for a given process, provided this corresponds to a region of validity for any of the other processes where Eq. (14) with $p_i = 0$ is a good approximation. From this it turns out that we can use Eq. (14) with $p_i = 0$ for any t (Ref. 8).

In practice we require that allowed couplings vanish only if they are required to do so by consistency with other processes and constraints. We also require secondary contributions to $[a]$ (backgrounds or other states which shift the effective average m_a away from the mass m_{aL} of the lowest contributing single-particle state) be as small as possible. In other words, we simultaneously minimize m_{aL} and $|m_a^2 - m_{aL}^2|$ in Eq. (14) with $p_i = 0$ for all the dominant channel processes, with 1,2,3,4 lying on leading Regge trajectories and $[a]$ having the lightest quark-mass content for a given output $\alpha(t)$ (Ref. 8).

In our calculations so far, we have used $\bar{s} - s_a = 1/2\alpha'$ and $p_1 = 0$ as explicit constraints on our parameters, with p_1 determined from Eqs. (13) and (11). We have also approximated the last four factors of Eq. (13) by a constant; this was found to have a relatively small effect on the quantities of physical interest in the explicit case of $\pi\pi$ scattering, with $v_c = \bar{v}_0$.

By applying the above procedure to Fig. 2 with π, ρ and their Regge recurrences for 1, 2, 3, 4, and α , we obtain

$$m_\pi^2 = m_\rho^2 - 1/2\alpha'_\rho = 0, \quad \alpha'_\pi = \alpha'_\rho = \text{const},$$

in good agreement with experiment. The results are very similar to the ones in Ref. 8, where α was approximated by α_1 , although m_a and c in Eq. (14) turned out to be somewhat different for low- S_m processes. We took the $\pi\pi \rightarrow \pi\pi$ Lovelace-Veneziano dual-resonance model¹⁰ result $3\alpha_{\rho_0}(0) = 1 - 4\alpha'_0 m_\pi^2$ with vanishing $(\alpha_{\rho_0} - 1)$ daughter. This gave

$$\alpha' = 1.1547\alpha'_0, \quad m_\rho^2 = 0.6495m_{\rho_0}^2.$$

The results are not sensitive to m_{π_0}/m_{ρ_0} , which we took from the quenched lattice calculations of Ref. 2 without any quark-mass extrapolation. Finally, the effect of g_2 is small in Eq. (11), thereby justifying Eq. (9), even though it corresponds to a fairly broad $y^{-\lambda} G(y)$ peak.

If we next apply our procedure to Fig. 2 with α_π, α_ρ states for 1 and 3 and α_N, α_Δ states for 2, 4, and α , we find, with $\alpha'_{\Delta_0} = \alpha'_{\rho_0} = \alpha'_{N_0}$,

$$m_\Delta^2 - 1/2\alpha'_\rho = m_N^2 = m_\rho^2 + 1/4\alpha'_\rho, \quad \alpha'_\Delta = \alpha'_N = \alpha'_\rho,$$

again in good agreement with experiment and insensitive to the values of m_{N_0} and m_{Δ_0} (Refs. 9 and 11), which we took from Ref. 2. Here the lowest (\bar{q}) line was replaced by a qq diquark in Fig. 1.

Our calculations show that most of the dynamics generating the leading-trajectory hadrons come from open hadronic channels. This is not, of course, necessarily in contradiction with primitive valence-quark models, but merely means that open hadronic channels play an important role in generating the final "confinement" forces binding such quarks. No *a priori* truncation or partial diagonalization of these channels was made in our scheme.

In the case of $\pi\pi$ scattering, we find that

$\Gamma_0(\infty) \ll \Gamma(\infty)$. This is consistent with the more detailed $\alpha \simeq \alpha_1$ results of Matute,¹² who found a $\Gamma(\infty)$ which is already consistent with experiment. Now Γ_0 is related to a HHH_0 coupling and so cannot be compared directly with the results of a (short-range) quenched-loop lattice calculation, for example, which can only give $H_0H_0H_0$ couplings. By applying some of our ($HH \rightarrow HH$) methods to $H_0H \rightarrow HH$ and $H_0H_0 \rightarrow HH$ processes, we can relate our HHH_0 couplings first to H_0HH_0 , and then to $H_0H_0H_0$ couplings.

Eventually, improved calculations would entail increasing values of m_c , with an addition to Fig. 2(a) equal to the negative of the $m < m_c$ exchange contribution of Figs. 2(b), etc., to avoid any double counting. The $m_c \rightarrow \infty$ limit is then not, however, equivalent to dropping the quark degrees of freedom.

In a more complete treatment of hadronic channels we

must deal explicitly with the hadron-loop integrals that come into Fig. 2(b), for example.^{8,12} This is in any case needed for heavy-quark situations, for which Eq. (7) may fail because of the presence of a high-mass scale, although alternative approximations may be possible, as in the model of Ref. 13, which gave effective logarithmic $c\bar{c}$ and $b\bar{b}$ potentials.

Finally, some of our methods may be applicable, perhaps in modified form, to an implementation of the compactification of superstrings. This is also a situation where one has different short-range (ten-dimensional)¹⁴ and long-range (four-dimensional) dynamics, and may even provide constraints which would help to select the correct compactification scheme.

This work was supported in part by the U.S. Department of Energy.

¹See, e.g., M. Mashaal, T. N. Pham, and T. N. Truong, Phys. Rev. Lett. **56**, 436 (1986).

²See, e.g., K. C. Bowler *et al.*, Phys. Lett. **162B**, 354 (1985).

³N. A. Törnqvist, Ann. Phys. (N.Y.) **123**, 1 (1979); Nucl. Phys. **B203**, 268 (1982).

⁴See, e.g., M. Park and P. B. Shaw, Phys. Rev. D **30**, 437 (1984).

⁵See, e.g., G. E. Brown and M. Rho, Phys. Today **36** (2), 24 (1983).

⁶See, e.g., M. Gell-Mann, Talk presented at the 1st Int. Congr. on the Hist. of Scientific Ideas, Catalunya, Spain (1983), California Institute of Technology Report No. CALT-68-1214 (unpublished).

⁷E. Witten, Nucl. Phys. **B160**, 57 (1979); **B223**, 422 (1983);

B223, 433 (1983); G. Adkins, C. Nappi, and E. Witten, *ibid.* **B228**, 552 (1983); J. L. Gervais and B. Sakita, Phys. Rev. Lett. **52**, 87 (1984); K. Bardakci, Nucl. Phys. **B243**, 197 (1984).

⁸L. A. P. Balázs, Phys. Rev. D **26**, 1671 (1982).

⁹L. A. P. Balázs, Phys. Lett. **120B**, 426 (1983).

¹⁰C. Lovelace, Phys. Lett. **28B**, 264 (1968).

¹¹L. A. P. Balázs and B. Nicolescu, Phys. Rev. D **28**, 2818 (1983).

¹²E. A. Matute, Phys. Rev. D **32**, 1205 (1985).

¹³L. A. P. Balázs, Phys. Rev. D **31**, 1648 (1985).

¹⁴See, e.g., L. A. P. Balázs, Phys. Rev. Lett. **56**, 1759 (1986).